

# Ultimate strength of stiffened plate girders subjected to shear

Autor(en): **Komatsu, Sadao**

Objektyp: **Article**

Zeitschrift: **IABSE reports of the working commissions = Rapports des commissions de travail AIPC = IVBH Berichte der Arbeitskommissionen**

Band (Jahr): **11 (1971)**

PDF erstellt am: **26.05.2024**

Persistenter Link: <https://doi.org/10.5169/seals-12052>

## **Nutzungsbedingungen**

Die ETH-Bibliothek ist Anbieterin der digitalisierten Zeitschriften. Sie besitzt keine Urheberrechte an den Inhalten der Zeitschriften. Die Rechte liegen in der Regel bei den Herausgebern.

Die auf der Plattform e-periodica veröffentlichten Dokumente stehen für nicht-kommerzielle Zwecke in Lehre und Forschung sowie für die private Nutzung frei zur Verfügung. Einzelne Dateien oder Ausdrucke aus diesem Angebot können zusammen mit diesen Nutzungsbedingungen und den korrekten Herkunftsbezeichnungen weitergegeben werden.

Das Veröffentlichen von Bildern in Print- und Online-Publikationen ist nur mit vorheriger Genehmigung der Rechteinhaber erlaubt. Die systematische Speicherung von Teilen des elektronischen Angebots auf anderen Servern bedarf ebenfalls des schriftlichen Einverständnisses der Rechteinhaber.

## **Haftungsausschluss**

Alle Angaben erfolgen ohne Gewähr für Vollständigkeit oder Richtigkeit. Es wird keine Haftung übernommen für Schäden durch die Verwendung von Informationen aus diesem Online-Angebot oder durch das Fehlen von Informationen. Dies gilt auch für Inhalte Dritter, die über dieses Angebot zugänglich sind.

## Ultimate Strength of Stiffened Plate Girders Subjected to Shear

Résistance à la ruine des poutres à âme pleine raidies soumises au cisaillement

Tragfähigkeit ausgesteifter, schubbeanspruchter Blechträger

SADAO KOMATSU

Dr. Eng.

Professor, Department of Civil Engineering  
Osaka University, Osaka, Japan

### I. INTRODUCTION

For many years it was recognized that the static strength of plate girder entirely depends upon the web buckling strength. However, it has been shown by Massonnet, Rockey, Basler and other authors having been in progress since 1957 that the slender-web plate girder has its considerable inherent post-buckling strength. In several countries, the current Design Specification for transversely stiffened plate girders is based on these findings.

The present effort is part of a continuing study about the behavior of slender-web plate girder stiffened by transverse and longitudinal stiffeners, and that is concerned with the predicting of the limit strength of its panel under shear. To insure the justification of this approach, a series of proof-tests was carried out at Osaka University in the summer of 1968.

Five 7m long welded girders with 3.33mm webs, the slenderness ratios of which were 200, 225, 250, were tested. The test panels of girders had one or two longitudinal stiffeners, dividing the web into two or three subpanels of equal depth, in addition to transverse stiffeners. The stiffeners were designed by taking Prof. Skaloud's recommendations so as to allow the sufficient development of incomplete diagonal tension field.

The behavior of longitudinally stiffened slender-web girder under shear will be discussed in this report. Then the essential data of the proof-tests were compared with the predicted values. These test results as well as ones measured by several authors show excellent agreement with theoretical values obtained according to proposed method.

Finally, design recommendations based on these static studies have been formulated for plate girders subjected to shear.

### II. MODE OF FAILURE UNDER SHEAR

A pure shear loading causes some kinds of failure mode chiefly dependent on the relation between the slenderness of web and the strength of smaller flange. In the case of low slenderness, a shear carrying action called "beam action" resists at the neutral axis to the pure shear. With the attainment of shear yield stress at the same place, the failure starts and then the yielding phenomenon spreads all over the web by only small increasing of the shear force. To design the girder having a comparatively slender web according to the classical beam theory based on "beam action", we need transverse stiffener spaced

close enough so that instability due to shear is excluded.

On the other hand, it has been long recognized that the pure diagonal tension develops in such a extremely thin web as those being seen in aircraft. The action of a pure diagonal tension field is quite similar to that of a diagonal member of Pratt Truss.

In the case of median slenderness, a pure shear loading results in equal tensile and compressive principal stresses up to critical shear buckling. After buckling, only a diagonal tension can carry any additional shear load. Basler and his colleagues at Lehigh University have developed "Theory of modified incomplete diagonal tension field". In the state of incomplete diagonal tension, two kinds of stress situation always exist together in the web plate. One of them corresponds to a critical shear stress, another a diagonal tensile stress. The mode of failure in this stress condition is greatly affected by the rigidity of the boundary members and the slenderness of web plate. If the boundary members have sufficient stiffness, the diagonal tensile stress will be uniformly distributed in the web plate. So the collapse of that panel certainly occurs due to yielding all over the web plate. If the boundary member, however, do not have sufficient rigidity, yield zone is restricted to a narrow diagonal strip. The diagonal strip of the web flows plastically with the development of plastic hinges in the flange. The residual flange and web deflections shown by Prof. Rockey make it quite clear that the mode of failure is not similar to that assumed by Baslar. It should be also noted that the position of plastic hinge varies with the flange stiffness, being quite differ from Fujii's assumption.

For high flange stiffness, the plastic hing is located in the middle point of the panel length. While, its position is quite near a corner of panel for relatively flexible flange.

### III. COMPUTING PROCEDURE

In order to find the ultimate strength of a plate girder under shear, the girder may be assumed to behave according to beam theory up to the critical buckling stress of web plate and then in a diagonal tension field manner up to the yielding point. With the exception of extremely low slenderness of web, for example less than 90, or extremely flexible stiffness of flange, the panel may also be assumed to be rigidly clamped along the flange.

Fig. 1 shows the relation between the extension of diagonal tension field and the deformation of panel-frame after collapse. In the same figure,  $\gamma$  denotes the shearing displacement and  $v(x)$  the deflection at a point  $x$  of flange due to its bending. If the tension field develops with the inclination  $\theta$  to girder axis after buckling, a tensile strain  $\epsilon_{tu}$  will be induced in the direction P'R' parallel to that of tension field.

$$\epsilon_{tu} = \left[ \gamma - \frac{v_u(x)}{a-x} \right] \sin \theta \cdot \cos \theta \quad (1)$$

, where  $a$  is the panel length.

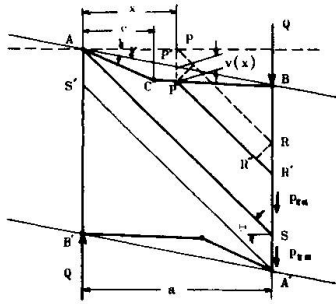


Fig. 1 Deformation of shear panel

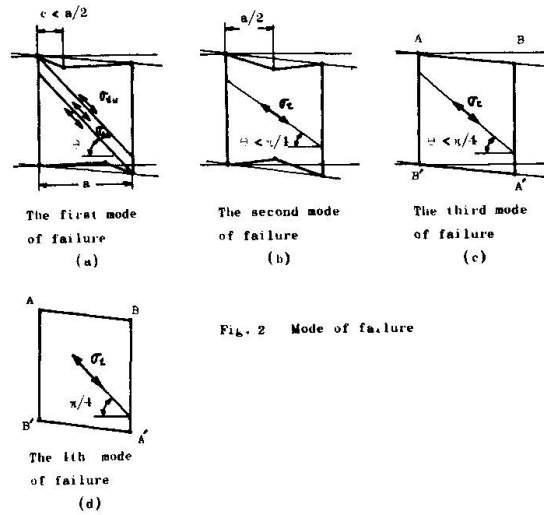


Fig. 2 Mode of failure

Corresponding tensile stress  $\sigma_{tu}$  will be also produced with the elastic modulus  $E_t$ .

$$\sigma_{tu} = E_t \left[ \gamma - \frac{V_u(x)}{a-x} \right] \sin \theta \cdot \cos \theta \quad (2)$$

Therefore, a distributed transverse internal force  $q_u$  acts on the flange all over the span AB.

$$q_u = E_t \left[ \gamma - \frac{V_u(x)}{a-x} \right] \sin^3 \theta \cdot \cos \theta \cdot t_w \quad (3)$$

, where  $t_w$  is the thickness of web plate.

Whereas it may be assumed that both bounds A'S and AS' are scarcely deformed, a diagonal tensile stress  $\sigma_{tm}$  in central region may be written as follows;

$$\sigma_{tm} = E_t \gamma \sin \theta \cdot \cos \theta \quad (4)$$

Now, two kinds of failure mode are considered according to the rigidity of flange. The first mode corresponding to a relatively flexible flange starts with bending collapse of flange, being accompanied by web-yielding in the central region such as shown in Fig.1. However, both upper region ABS and lower one A'B'S' remain elastic in spite of failure of girder. Neglecting the elastic deformation, the deflection of flange just after collapse may be represented by the following linear equation of coordinate  $x$ .

$$\begin{aligned} v(x) &= \frac{x}{c} \Delta & 0 \leq x \leq c \\ v(x) &= \frac{a-x}{a-c} \Delta & c \leq x \leq a \end{aligned} \quad (5)$$

Substituting  $v(x)$  into eq.(3), the transverse internal force  $q_u$  is written by

$$\begin{aligned}
q_u &= E_t \left( \gamma - \frac{x}{c} \cdot \frac{\Delta}{a-x} \right) \sin^3 \theta \cdot \cos \theta \cdot t_w \quad 0 \leq x \leq c \\
q_u &= q_{u2} = E_t \left( \gamma - \frac{\Delta}{a-c} \right) \sin^3 \theta \cdot \cos \theta \cdot t_w \quad c \leq x \leq a
\end{aligned} \quad (6)$$

, where  $\Delta$  is the deflection at the point C.  
Especially, at  $x=0$

$$q_u = q_{u1} = E_t \gamma \sin^3 \theta \cdot \cos \theta \cdot t_w \quad (7)$$

For the sake of simplicity, the linear distribution of transverse internal force  $q_u$  along the coordinate axis  $x$  may be assumed as an approximation between A and C.

$$q_u = q_{u1} - (q_{u1} - q_{u2}) \frac{x}{c} \quad (0 \leq x \leq c) \quad (8)$$

By applying the principle of virtual displacement to the flange AB broken off by the transverse action  $q_u$ , a following relation can be obtained.

$$\frac{12a}{c(a-c)} M_p = c q_{u1} + (3a-c) q_{u2} \quad (9)$$

, where  $M_p$  denotes the full plastic moment of smaller flange, being computed by following formula.

$$M_p = \frac{1}{4} \sigma_{fy} b_f t_f^2 \quad (10)$$

In above formula,  $\sigma_{fy}$ ,  $b_f$ , and  $t_f$  denote yield stress, breadth, and thickness of flange, respectively

Substituting eqs.(6) and (7) into eq.(9), and putting

$$\begin{aligned}
\bar{\eta} &= E_t \Delta \sin^3 \theta \cos \theta \cdot t_w / a \\
&= \frac{q_{u1}(a-c) - \frac{4M_p}{c}}{a - \frac{c}{3}}
\end{aligned} \quad (11)$$

Considering of equilibrium in vertical direction at the cross section AB gives a following relation,

$$Q = \int_0^a p_{zu}(x) dy(x) + \int_{a \tan \theta}^b p_{zm}(y) dy + \tau_{cr} b t_w \quad (a)$$

,  $p_{zu}$  and  $p_{zm}$  are shear internal forces per unit length along the boundary at the upper and central region, respectively as shown in Fig.1. The third term represents the contribution of remaining beam action. From boundary conditions of the panel,

$$\left. \begin{aligned} p_{zu} &= \sigma_{tu} \sin \theta \cdot \cos \theta \cdot t_w \\ p_{zm} &= \sigma_{tm} \sin \theta \cdot \cos \theta \cdot t_w \end{aligned} \right\} \quad (12)$$

Then, using eqs.(12) in eq.(a),

$$Q = q_{ul} b \cot \theta - \bar{l} \left[ 1 + \frac{c}{2(a-c)} \right] a + \tau_{cr} b t_w \quad (13)$$

Furthermore, the attainment of yielding in the central region causes the complete failure of plate girder, so that the diagonal tensile stress  $\sigma_{tm}$  can increase up to following value according to the yield criterion,

$$\sigma_{tm} = \sigma_{wy} - 2 \tau_{cr} \sin 2 \theta \quad (14)$$

, where  $\sigma_{wy}$ ,  $\tau_{cr}$  are yield stress and critical shear buckling stress of web, respectively.

So  $q_{ul}$  becomes as follows,

$$q_{ul} = (\sigma_{wy} - 2 \tau_{cr} \sin 2 \theta) \sin^2 \theta \cdot t_w \quad (15)$$

Substituting eqs.(11) and (15) into eq.(13), the ultimate shear force can be finally obtained.

$$\begin{aligned} Q &= \frac{1}{2} (\sigma_{wy} - 2 \tau_{cr} \sin 2 \theta) \{ b \sin 2 \theta - \alpha (1 - \cos 2 \theta) \} t_w \\ &\quad + \frac{4 M_p \alpha}{c(a-c)} + \tau_{cr} b t_w \end{aligned} \quad (16)$$

, where  $b$  and  $t_w$  are depth and thickness of web plate respectively, and

$$\alpha = \frac{a-c/2}{a-c/3} a \quad (17)$$

The inclination of diagonal tension field  $\theta$  can be obtained under such condition as the shearing resistance should become maximum; that is,

$$\frac{\partial Q}{\partial \theta} = 0$$

, from which the following relation is deduced.

$$\begin{aligned} &\sigma_{wy} (b \cos 2 \theta - \alpha \sin 2 \theta) + 2 \tau_{cr} \{ \alpha (\cos 2 \theta - \cos 4 \theta) \\ &\quad - b \sin 4 \theta \} = 0 \end{aligned} \quad (18)$$

For this case, the inclination should be determined to satisfy above condition (18).

Then the position of plastic hinge can be determined by a following empirical formula,

$$C = \frac{1.782 \frac{M_p}{\sigma_{wy} b^2 t_w} + 0.38}{2(1.782 \frac{M_p}{\sigma_{wy} b^2 t_w} + 1)} \quad a \quad (19)$$

For flexible flange,  $M_p$  value is so small that the factor  $\bar{\eta}$  of plastic deflection in eq.(11) takes positive value. In such a case, the first mode of collapse as shown in Fig.2(a) will be occurred. If the rigidity and strength of flange are much enough to resist elastically against the transverse internal force  $q_u$  even after yielding of web, the third or fourth mode of failure will be deduced as shown in Fig.2(c) or (d). In these modes, the diagonal tensile stress will be uniformly distributed all over the panel. The failure of girder will be induced by complete panel-yielding, when the diagonal tensile stress  $\sigma_t$  will attain to the yield point. Therefore

$$\begin{aligned} p_z = p_{zu} = p_{zm} &= \sigma_t \sin \theta \cdot \cos \theta \cdot t_w \\ &= \frac{1}{2} (\sigma_{wy} - 2 \tau_{cr} \sin 2\theta) \sin 2\theta \cdot t_w \end{aligned} \quad (20)$$

Substituting eq.(20) into eq.(a), the ultimate shear force  $Q$  can be obtained as follows,

$$Q = \left\{ \frac{1}{2} \sigma_{wy} \sin 2\theta + \tau_{cr} (1 - \sin^2 2\theta) \right\} b t_w \quad (21)$$

According to the condition of maximum value  $\partial Q / \partial \theta = 0$  again,

$$\cos 2\theta (\sigma_{wy} - 4 \tau_{cr} \sin 2\theta) = 0 \quad (22)$$

If the slenderness of web is so large that the critical shear buckling stress has a very small value and an inequality

$$\sigma_{wy} - 4 \tau_{cr} \geq 0 \quad (23)$$

can be satisfied, the fourth mode of failure will be occurred. Since the inclination  $\theta$  of tension field should become  $\pi/4$  in such a case, the ultimate shear force  $Q$  can be readily found.

$$Q = \tau_{wy} b t_w + 4M_p/a \quad (24)$$

The last term represents the sum of the full plastic moments at the corners A, B, A' and B'.

This means so-called Wagner's complete tension field.

However, if the slenderness of web plate is not so large as to satisfy inequality(23), the inclination should be determined by a following equation.

$$\theta (= \theta_0) = \frac{1}{2} \sin^{-1} \frac{\sigma_{wy}}{4\tau_{cr}} \quad (25)$$

The ultimate force  $Q$  should be, of course, calculated by eq.(21). Consequently the third mode of failure will be occurred in such a case.

As an intermediate case between the first and third mode, it will be considered that the plastic hinge at the middle point of flange will be built up simultaneously with the spreading of yielded scope in the web. For such a case, the mode of failure may be called the second mode and shown in Fig.2(b). In this case,  $\bar{\eta}$  takes a negative value for  $\theta$  satisfying condition(18), while it has positive one for  $\theta$  taking  $\pi/4$  in spite of satisfying inequality(23).

Since it must be complicated to analyze rigorously such stress situation, the following approach may be useful to find ultimate load. From the condition of simultaneous collapse, the following relation may be derived.

$$M_p = \frac{a^2}{16} (\sigma_{wy} - 2\tau_{cr} \sin 2\theta) \sin^2 \theta \cdot t_w \quad (26)$$

When the plastic moment  $M_p$  of flange is given, the inclination  $\theta$  for such mode of failure should satisfy above eq.(26).

Thus eq.(21) can be applied again to determine the ultimate shear force, because the combined stress will be attained to yield point in entire panel immediately after collapse of flange.

The practical computing process may be carried out in such a way as shown by a block diagram as shown in Fig.3.

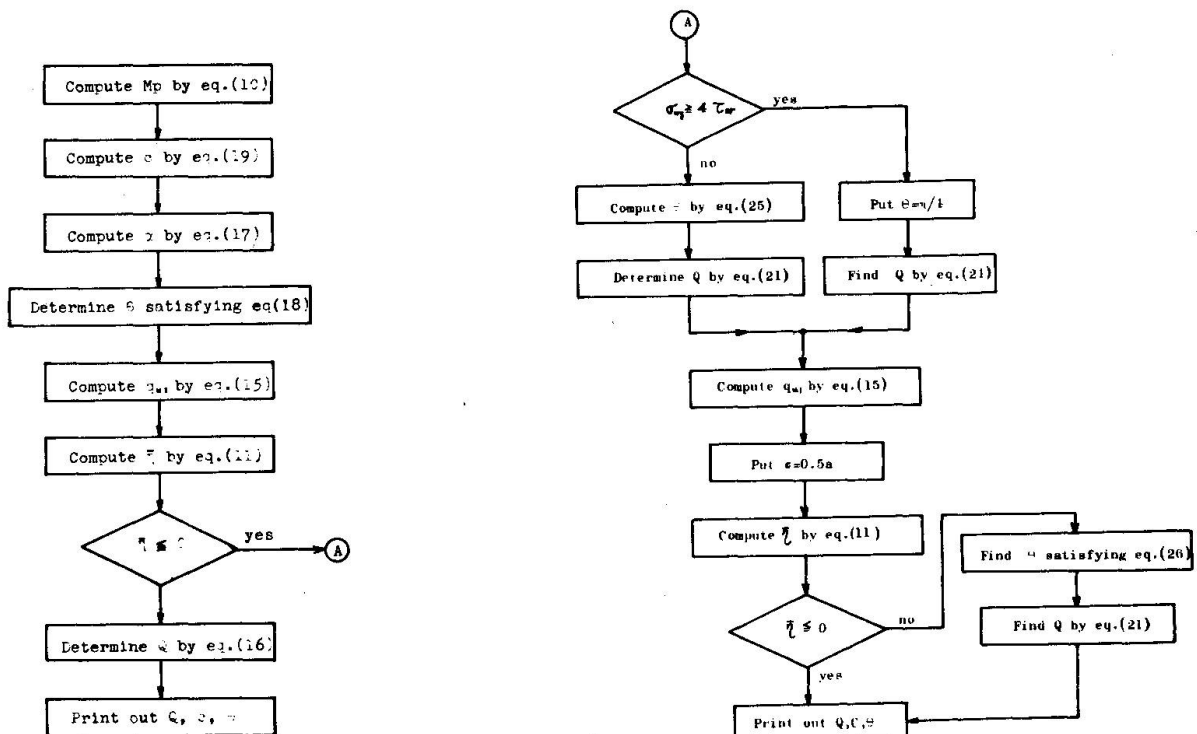


Fig. 3 Block diagram for ultimate shear force computation program



#### IV. PROOF TESTS

The primary purpose of the main tests was to justify the newly developed theory for the ultimate strength of unsymmetrical plate girder under shear.

Five girders could be loaded statically to fail for this purpose. Since it was undesirable to fail in any panel other than the test-panel, the girder was designed so that the failure loads were remarkably different for adjacent panels.

##### 4.1 Girder Specimens

Among the five girders tested, each of three girders had a one-sided longitudinal stiffener at the middle of web depth shown in Fig.4, the other had two one-sided longitudinal stiffeners on the internal trisector of the web. The test girders were connected to a rigid supporting girder by high tension bolts shown in Fig.5.

Moreover, two corner plates were welded to increase the rigidity of upper flange shown in Fig.6. The dimensions of test girders are given in Table 1.

##### 4.2 Test Load

The load was applied by means of two oiljacks with total capacity 150tons. Five equal increments of load were taken up to two-thirds of predicted yield load, then the load was increased by 2tons at one time until failure.

##### 4.3 Material Properties

The actual dimensions of the component plates of the test specimens were obtained from measurements on coupon plates cut from the various plates before fabrication. Table 2 shows the measured values of dimensions and the results of the tensile tests.

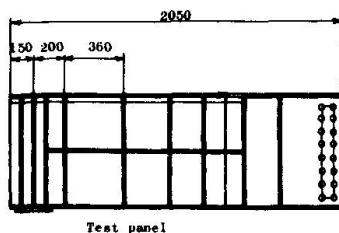


Fig. 4 Specimen A-2

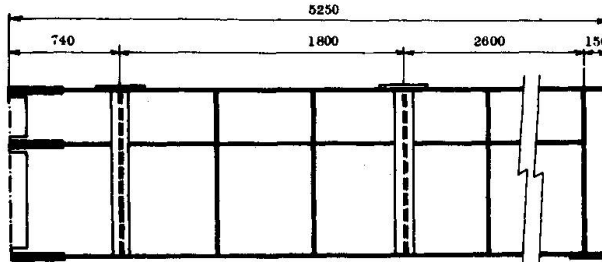


Fig. 5 Supporting girder

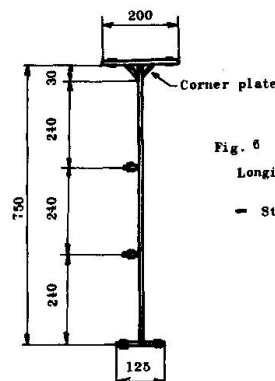


Fig. 6 Specimen A-3  
Longitudinal stiffener section  
35mm=1.5mm  
— Strain gauge

Specimen	b cm	b <sub>1</sub> cm	t <sub>w</sub> cm	b <sub>2</sub> cm	t <sub>f</sub> cm	a cm	n
A-1	67	32	0.333	12.5	1.0	32	1
A-2	75	36	0.333	12.5	1.0	36	1
A-3	75	24	0.333	12.5	1.0	36	2
A-4	83	40	0.333	12.5	1.0	40	1
A-5	83	28.7	0.333	12.5	1.0	40	2

b: depth of web  
 b<sub>1</sub>: depth of subpanel  
 t<sub>w</sub>: thickness of web  
 b<sub>2</sub>: breadth of smaller flange  
 t<sub>f</sub>: thickness of smaller flange  
 a: length of shear panel ( distance between transverse stiffeners )  
 n: number of longitudinal stiffeners

Table 1 Dimension of panel

Specimen	Size	Section area	Gauge distance	Yield load ton	Ultimate load ton	Yield stress kg/cm	Ultimate stress kg/cm	Stretch	Percent-stretch
A-1	39.93 9.93	396.505	200	15.00	21.11	3783.1	5399.7	44.0	22.0
A-2	39.95 9.85	393.508	200	14.89	21.06	3784.0	5352.0	45.0	22.5
A-3	40.00 9.65	386.000	200	14.50	20.69	3756.9	5360.1	41.0	20.5
B-1	40.07 10.69	428.348	200	15.93	24.02	3719.4	5608.2	41.0	20.5
B-2	40.07 10.79	432.355	200	15.98	24.16	3695.7	5588.1	41.0	20.5
B-3	39.87 10.61	423.021	200	16.00	23.80	3782.5	5626.2	41.0	22.5
C	50.03 14.09	704.923	200	25.70	40.10	3646.0	5688.8	44.0	22.0
D	25.25 4.44	112.110	50	5.50	6.46	4906.3	5762.2	10.5	21.0
E-1	23.17 3.33	77.156	50	3.50	4.35	4533.7	5637.9	16.5	33.0
E-2	23.20 3.35	77.72	50	3.29	4.19	4233.1	5391.1	15.5	31.0
E-3	23.17 3.33	77.156	50	3.27	4.19	4237.9	5430.6	16.0	32.0

A, B, C, D: SM50 for flange E: SM50 for web

Table 2 Tensile test of material

## V. TEST RESULTS

In this paper, the typical data of many test results are shown as follows.

### 5.1 Deflection of Web

The lateral deflections at the middle point of each subpanel under shear were plotted against load as shown in Fig.7.

### 5.2 Strain of Flanges

The longitudinal strain of both flanges were plotted against load as shown in Fig.8. It can be considered that these strains were suddenly increased due to shear buckling of web plate. Therefore, actual critical shear buckling stresses may be observed from these diagrams. Thus, the experimental critical shear stresses could be seen to coincide with the theoretical ones of subpanel fixed at both longitudinal sides and simply supported at vertical sides.

### 5.3 Deflection of Girders

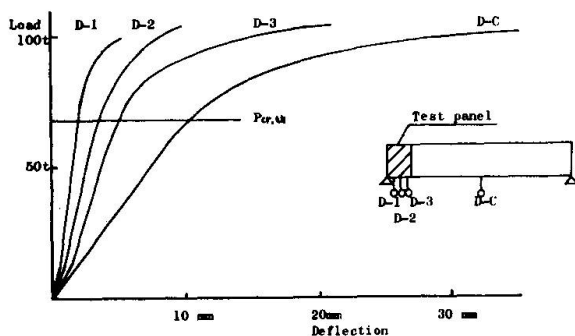


Fig. 9 Vertical deflection of girder A-2

The deflection of several points measured by dialgages were plotted against loads as shown in Fig.9. Most curves tend to deviate from a straight line just after predicted critical shear buckling load  $P_{cr,th}$  as shown in the same figures. From these facts, the theoretical values for shear buckling can be considered to be acceptable.

### 5.4 Strain of Longitudinal Stiffeners

The strains of longitudinal stiffeners were plotted against applied load as shown in Fig.10. After buckling of web, the longitudinal stiffeners of all test girders, except A-4, were bent upward. This behavior was caused by the fact that the membrane were pull up towards the upper flange which was more rigid than the lower one. Moreover, the longitudinal strains at the opposite side to stiffened surface of web were compressive in the case of one stiffener, or compressive at upper stiffener and tensile at lower one in the case of two stiffeners.

### 5.5 Strain of Transverse Stiffener

The strains of transverse stiffeners were plotted against applied load as shown in Fig.11. The strain scarcely induced in any transverse stiffener up to web buckling. The strain of transverse stiffeners as well as flanges, however, abruptly increase after buckling of web, because the frame consisting of flanges and stiffeners must bear the internal forces transferred from the buckled web.

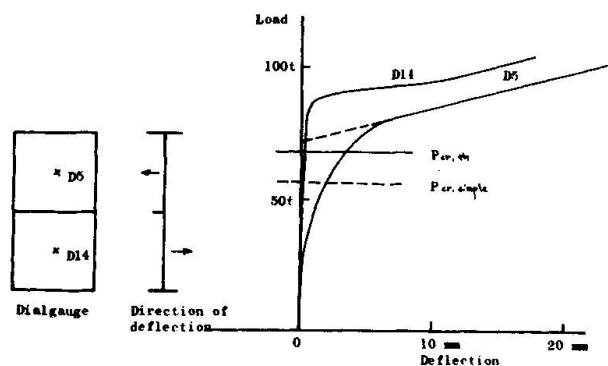


Fig. 7 Web deflection A-2

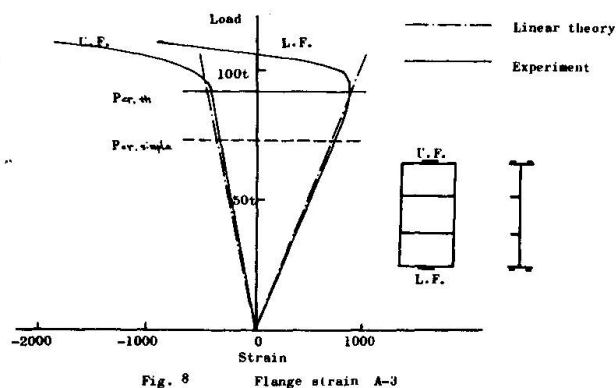


Fig. 8 Flange strain A-3

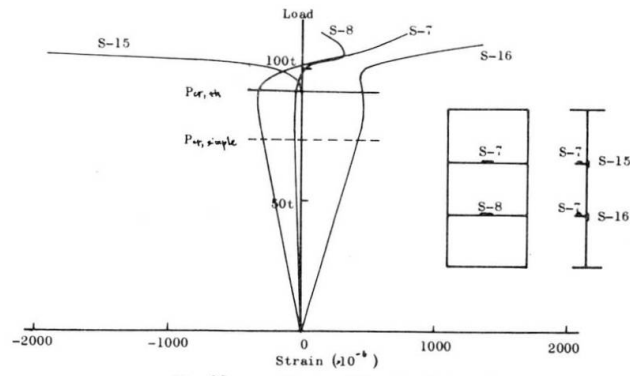


Fig. 10 Strain of longitudinal stiffeners

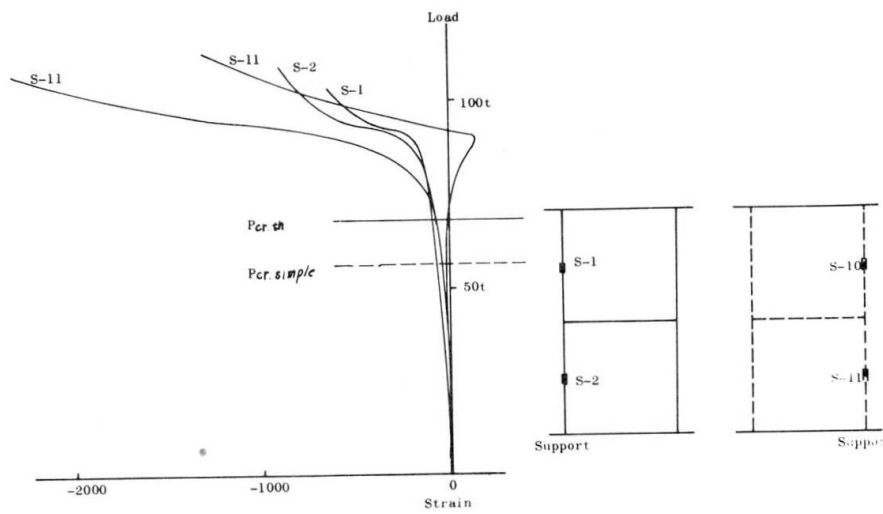
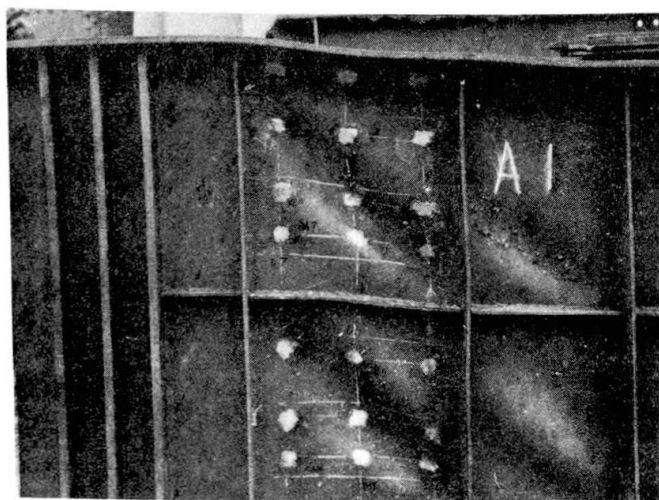
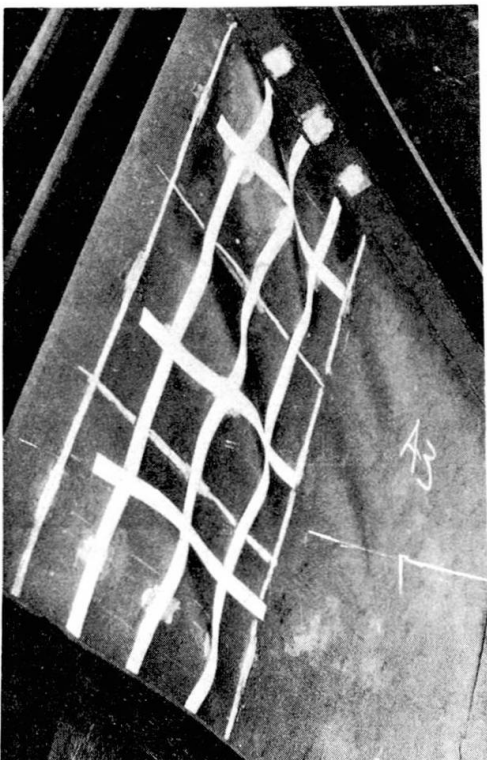


Fig. 11 Strain of transverse stiffener A-2



## VI. COMPARISON BETWEEN PREDICTED VALUES AND EXPERIMENTAL RESULTS

The experimentally obtained ultimate load  $Q_{ex}$  were compared with the values  $Q_{th}$  based on the author's theory as shown in Table 3. It can be seen that the fairly agreement between them could be obtained.

Moreover, the strength of every stiffeners except A-4 girder may be recognized to be so enough as to resist elastically diagonal tensile stress.

In Table 3, the experimental results given by other authors also agree with author's theoretical values.

## VII. REQUIREMENT FOR FLANGE STRENGTH

In order to establish a well balanced design of girder under shear, how large flange or stiffener should be adopted? Concerning with this problem, it is rational to choose such a flange as to make the girder fail in the second mode for given dimension of web plate.

Hence, for the web satisfying inequality (23), the maximum ultimate shear force  $Q_{max}$  can be given when  $\theta$  is equal to  $\pi/4$ , that is

$$Q_{max} = \tau_{wy} b t_w + 4M_p/a \quad (27)$$

Herein, the required plastic moment  $M_{p,req}$  of smaller flange may be given from eq(26) as follows,

$$M_{p,req} = \frac{a^2}{32} (\sigma_{wy} - 2\tau_{cr}) t_w \quad (28)$$

However, if inequality(23) cannot be satisfied for given web, the inclination  $\theta = \theta_0$  should be decided by eq.(25). Therefore,  $Q_{max}$  takes the value given by substituting  $\theta = \theta_0$  into eq.(21). In this case, a required plastic moment  $M_{p,req}$  of flange should be found by a following formula.

$$M_{p,req} = \frac{a^2}{16} (\sigma_{wy} - 2\tau_{cr} \sin 2\theta_0) \sin^2 \theta_0 t_w \quad (29)$$

The required full plastic moments  $M_{p,req}$  of desirable flange for girder specimens can be compared with the actual ones  $M_{p,act}$  in Table 3. The strength of flange in the girder at which the 3rd mode of failure was occurred was too large to be appropriately and economically designed for designated web. While, in the girder collapsing in the 1st mode, the strength of flange was too small to use up the full strength of girder.

## CONCLUSIONS

An approach to the limit design of thin-web plate girder with transverse and longitudinal stiffeners under shear was proposed in this paper. It was shown by analysis that there were four modes of failure any one of which would

be induced in accordance with the relative strength of flange to the web. This calculating method of ultimate strength includes both the finding of the mode of failure for designated dimension of member and the determination of ultimate strength.

It was shown that the test results given by several authors fairly agreed with the theoretical ones.

The rational design method of shear panel, especially the determination of desirable dimension of flange was indicated here.

The stiffness of longitudinal stiffener has only to be sufficient to increase the critical buckling stress as much as possible and make the stiffener remain straight up to the collapse load of girder.

#### REFERENCES

1. Ch. Massonnet,  
Stability considerations in the design of plate girders.  
Proce ASCE, vol. 86, ST 1, 1960.
2. Owen D.R.J., K.C. Rockey, and M. Skaloud,  
Behaviour of longitudinally reinforced plate girders.  
Prel. publication of 8th congress IABSE, 1968.
3. Rockey, K.C. and M. Skaloud,  
Influence of flange stiffness upon the load carrying capacity of webs in shear  
Prel. publication of 8th congress IABSE, 1968.
4. Ostapenko, A., B.T. Yen, and L.S. Beedle,  
Research on plate girders at Lehigh University.  
Prel. publication of 8th congress IABSE, 1968.
5. Fujii, T,  
On improved theory for Dr. Basler's theory  
Prel. publication of 8th congress IABSE, 1968.
6. Basler, K,  
Strength of plate girders in shear,  
Proce. ASCE vol. 87, ST 7, 1961.
7. Basler, K., Yen, B.T., Mueller, J.A., and Thürlimann, B.  
Web buckling tests on welded plate girders,  
Bulletin No. 64, Welding Research Council 1960.
8. Konishi I,  
Theories and experiments on the load carrying capacity of plate girders  
Report of Research Committee of Bridges, Steel Frames and Welding in  
Kansai District in Japan 1965.
9. Cooper, P.B.,  
Strength of longitudinally stiffened plate girders,  
Proc. ASCE, vol. 93, ST 2, 1967.
10. Patterson, P.J., J.A. Corrado, J.S. Huang, and B.T. Yen,  
Proof-tests of two slender-web welded plate girders,  
Fritz Engineering Laboratory Report No.327.7, 1969.
11. Schueller, W., and A. Ostapenko,  
Static tests on unsymmetrical plate girders main test series  
Fritz Engineering Laboratory Report No.328.6, 1968.
12. Skaloud, M.,  
Design of webplates of steel girders with regard to the postbuckling  
behaviour approximate solution  
The Structural Engineer vol. xxxx, No. 9, 1962.

	Specimen	Web			Flange			a	Plastic hinge C	Mode of failure	cr, th
		b (b <sub>1</sub> )	tw	Vwy	bf	tf	Vfy				
1	A-1	67 (32)	0.333	4,534	12.5	1.0	3,783	32	None	3rd	1758
	A-2	75 (36)	0.333	4,233	12.5	1.0	3,784	36	None	3rd	1555
	A-3	75 (24)	0.333	4,235	12.5	1.0	3,756	36	None	3rd	1842
	A-4	83 (40)	0.333	4,395	12.5	1.0	3,738	40	20.0	2nd	1450
	A-5	83 (27)	0.333	4,238	12.5	1.0	3,738	40	None	3rd	1769
2	TG-1	100	0.25	2,037	16	0.506	2,862	100	19.0	1st	145.8
	TG-1'	100	0.25	2,037	16	0.526	2,862	100	19.0	1st	145.8
	TG-2	100	0.25	2,037	20	1.008	2,862	100	19.2	1st	145.8
	TG-2'	100	0.25	2,037	20	1.012	2,862	100	19.2	1st	145.8
	TG-3	100	0.25	2,037	20	1.643	2,862	100	50.0	2nd	145.8
	TG-3'	100	0.25	2,037	20	1.642	2,862	100	50.0	2nd	145.8
	TG-4	100	0.25	2,037	20	2.016	2,862	100	50.0	2nd	145.8
	TG-4'	100	0.25	2,037	20	2.013	2,862	100	50.0	2nd	145.8
	TG-5	100	0.25	2,037	25	2.975	2,862	100	None	4th	145.8
	TG-5'	100	0.25	2,037	25	2.972	2,862	100	None	4th	145.8
3	G6-T1	127	0.49	2,580	30.8	1.975	2,665	190.5	36.6	1st	306
	G6-T2	127	0.49	2,580	30.8	1.975	2,665	95.2	47.6	2nd	435
	G6-T3	127	0.49	2,580	30.8	1.975	2,665	63.4	None	3rd	741
	G7-T1	127	0.498	2,580	30.95	1.95	2,645	127	24.4	1st	358
	G7-T2	127	0.498	2,580	30.95	1.95	2,645	127	24.4	1st	358
	G8-T1	127	0.50	2,630	30.45	1.902	2,910	381	73.2	1st	283
	G9-T1	127	0.333	3,130	30.45	1.902	2,940	381	73.4	1st	125
	G9-T2	127	0.333	3,130	30.45	1.902	2,940	190.5	36.7	1st	145
4	B	120	0.45	5,000	24.0	1.2	5,000	120	22.9	1st	328
5	F10-P1	127	0.665	2,405	39.5	3.20	1,915	190.3	95.2	2nd	579
	F10-P5	127	0.653	2,720	40.75	2.54	2,025	152.4	76.2	2nd	590
	F11-P3	240(193)	0.665	2,405	35.9	3.20	1,915	241	46.0	1st	262
	F11-P1	241(193)	0.66	2,405	36.0	3.18	1,738	335	64.0	1st	236
6	LS3-T1	127(85)	0.46	2,690	36	3.84	2,095	190	95	2nd	556

	Specimen	Longitudinal stiffener	$Q_{ex} \times 10^3$	$Q_{th} \times 10^3$	$Q_{ex}/Q_{th}$	$M_p, req.$	$M_p, act$
1	A-1	1	56.5	55.5	1.02	$5.692 \times 10^3$	$1.182 \times 10^4$
	A-2	1	57.5	56.8	1.01	$7.630 \times 10^3$	$1.183 \times 10^4$
	A-3	2	59.0	61.2	0.96	$5.191 \times 10^3$	$1.174 \times 10^4$
	A-4	1	63.0	63.0	1.00	$1.271 \times 10^4$	$1.168 \times 10^4$
	A-5	2	63.5	66.4	0.96	$7.025 \times 10^3$	$1.168 \times 10^4$
2	TG-1	0	15.54	14.09	1.10	$1.364 \times 10^5$	$2.931 \times 10^3$
	TG-1'	0	11.85	14.15	0.84	$1.364 \times 10^5$	$3.167 \times 10^3$
	TG-2	0	16.3	16.98	0.96	$1.364 \times 10^5$	$1.454 \times 10^4$
	TG-2'	0	14.15	17.01	0.83	$1.364 \times 10^5$	$1.466 \times 10^4$
	TG-3	0	19.4	19.32	1.00	$1.364 \times 10^5$	$3.863 \times 10^4$
	TG-3'	0	19.35	19.32	1.00	$1.364 \times 10^5$	$3.858 \times 10^4$
	TG-4	0	22.3	21.86	1.02	$1.364 \times 10^5$	$5.816 \times 10^4$
	TG-4'	0	21.1	21.86	0.97	$1.364 \times 10^5$	$5.799 \times 10^4$
	TG-5	0	31.47	31.78	0.99	$1.364 \times 10^5$	$1.583 \times 10^5$
	TG-5'	0	30.5	31.78	0.96	$1.364 \times 10^5$	$1.580 \times 10^5$
3	G6-T1	0	52.5	50.6	1.03	$1.005 \times 10^6$	$8.004 \times 10^4$
	G6-T2	0	68.0	70.4	0.97	$2.373 \times 10^5$	$8.004 \times 10^4$
	G6-T3	0	80.4	81.0	0.99	$4.038 \times 10^4$	$8.004 \times 10^4$
	G7-T1	0	63.5	65.9	0.96	$4.677 \times 10^5$	$7.782 \times 10^4$
	G7-T2	0	65.8	65.9	1.00	$4.677 \times 10^5$	$7.782 \times 10^4$
	G8-T1	0	38.6	36.5	1.06	$4.796 \times 10^6$	$8.014 \times 10^4$
	G9-T1	0	21.8	21.4	1.02	$4.349 \times 10^6$	$8.096 \times 10^4$
	G9-T2	0	34.0	36.2	0.94	$1.072 \times 10^6$	$8.096 \times 10^4$
4	B	0	76.0	78.7	0.97	$8.798 \times 10^5$	$4.320 \times 10^4$
5	F10-P1	0	83.5	88.1	0.95	$9.389 \times 10^5$	$1.936 \times 10^5$
	F10-P5	0	86.2	92.8	0.93	$7.303 \times 10^5$	$1.331 \times 10^5$
	F11-P3	1	127.5	128.9	0.99	$2.271 \times 10^6$	$1.760 \times 10^5$
	F11-P1	1	111.9	105.5	1.06	$4.472 \times 10^6$	$1.582 \times 10^5$
6	LS3-T1	1	63.5	71.3	0.89	$8.190 \times 10^5$	$2.780 \times 10^5$

b1 : Depth of main subpanel

C : Distance between plastic hinge and the nearest corner of panel

$M_p, req.$  : Required plastic moment of desirable flange for given web

$M_p, act$  : Existing plastic moment of flange

(1) Komatsu

(2) Skaloud

(3) Basler

(4) Konishi

(5) Patterson

(6) Cooper

\* mean value of twin specimens

unit : cm, kg

SADAO KOMATSU

Table 3 Comparison between experimental and theoretical ultimate load.



```

1      REAL NU,KS,MU,MP,MS
2      E=2.1*10.0**6
3      NU=0.3
4      PAI=3.141592
5      DO 100 J=1,21
6          READ(5,1000) B,B1,TW,SWY,BF,TF,SFY,A
7      1000  FORMAT(8F8.0)
8          READ(5,1001) KS,SK
9      1001  FORMAT(2F8.0)
10         ASP=A/B
11         TWY=0.5*SWY
12         WRITE(6,2000) B,TW,SWY,BF,TF,SFY,A
13     2000  FORMAT(1H,4H B=F8.2,4H TW=F8.2,5H SWY=F8.2,4H BF=F8.2,4H TF=F8.2
14           1,4H SF=F8.2,4H A=F8.2)
14         TCS=SK*PAI**2*E/12.0/(1.0-NU**2)*(TW/B1)**2
15         IF(TCS=0.5*TWY) 20,20,21
16     21    TCS=TWY*(1.0-3.0*(1.0-NU**2)/SK/PAI**2/E*TWY*(B1/TW)**2)
17     20    CONTINUE
18         TCR=KS*PAI**2*E/12.0/(1.0-NU**2)*(TW/B1)**2
19         IF(TCR=0.5*TWY) 10,10,11
20     11    TCR=TWY*(1.0-3.0*(1.0-NU**2)/KS/PAI**2/E*TWY*(B1/TW)**2)
21     10    WRITE(6,2001) TCR,TCS
22     2001  FORMAT(1H,4HTCR=F8.2,13X,4HTCS=F8.2)
23         MP=0.25*SFY*BF*TF**2
24         C=(0.38+1.782*MP/SWY/B**2/TW)*0.5/(1.0+1.782*MP/SWY/B**2/TW)*A
25         CA=C/A
26         ALP=(A-C/2.0)/(A-C/3.0)*A
27         II=1
28     52    T=0.10
29         JJ=1
30         BB=0.0
31         STEP=0.01
32         NC=1
33     1    T=T+STEP
34         GO TO (2,3),II
35     2    AA=SWY*(B*COS(2.0*T)-ALP*SIN(2.0*T))+2.0*TCR*(ALP*(COS(2.0*T)-COS
36           1(4.0*T))-B*SIN(4.0*T))
37     3    AA=MP-A**2/16.0*(SWY-2.0*TCR*SIN(2.0*T))*SIN(T)**2*TW
38     4    CC=AA*BB
39         IF(CC,LT,0.0) GO TO 5
40         BB=AA
41         NC=NC+1
42         IF(NC,GT,100) GO TO 7
43         GO TO 1
44     5    T=T-STEP
45         JJ=JJ+1
46         IF(JJ,EQ,3) GO TO 6
47         STEP=STEP/10.0
48         GO TO 1
49     6    T=T+0.5*STEP
50     7    CONTINUE
51         TH=T
52         GO TO (18,19),IT
53     18    CONTINUE
54     50    QU1=(SWY-2.0*TCR*SIN(2.0*TH))*SIN(TH)**2*TW
55     51    ETB=(QU1*(A-C)-4.0*MP/C)/(A-C/3.0)
56         IF(ETB) 12,12,13
57     13    CONTINUE
58         WRITE(6,2004)
59     2004  FORMAT(1H,11X,8H1ST MODE)
60         Q=0.5*(SWY-2.0*TCR*SIN(2.0*TH))*(B*SIN(2.0*TH)-ALP*(1.0-COS(2.0*
61           1TH)))*TW
62         Q=Q+4.0*MP*ALP/C/(A-C)+TCR*B*TW
63     C    OUT PUT
64     53    TUL=Q/B/TW
65         MU=TUL/TCR
66         TH=TH*180.0/PAI
67         IF(SWY-4.0*TCR) 22,23,23
68     22    X=SWY/4.0/TCR
69         TT=0.5*ATAN(X/SGHT(1.0-X**2))
70         STM=(SWY-2.0*TCR*SIN(2.0*TT))
71         PP=A**2/16.0*STM*SIN(TT)**2*TW
72         GO TO 60
73     23    STM=SWY-2.0*TCR
74         PP=A**2/32.0*STM*TW
75     60    CONTINUE
76         WRITE(6,2002) MP,PP,ALP,QU1,ETB
77     2002  FORMAT(1H,3HMP=E14.7,8H MP,REQ=E14.7,4X,4HALP=E15.7,6X,4HQU1=E15.
78           17,4X,4HETB=E15.7)
79         WRITE(6,2005) Q,C,TH,TUL,MU
80     2005  FORMAT(1H,2HQ=E15.7,5X,2HC=E15.7,5X,3HTH=E15.7,5X,5HTUL=E15.7,5X

```

```

1.3HMU=F15.7///)
78 WRITE(6,2003)
79 2003 FORMAT(///)
80 GO TO 56
81 12 IF(SWY-4.0*TCR) 14,15,15
82 14 X =SWY/4.0/TCR
83 TH =0.5*ATAN(X/SQRT(1.0-X**2))
84 Q =(0.5*SWY*SIN(2.0*TH)+TCR*(1.0-SIN(2.0*TH)**2))*B*TW
85 GO TO 54
86 15 TH =PAI/4.0
87 Q =TWY*B*TW +4.0*MP/A
88 54 QU1=(SWY-2.0*TCR*SIN(2.0*TH))*SIN(TH)**2*TW
89 C =0.5*A
90 ETB=(QU1*(A-C)-4.0*MP/C)/(A-C/3.0)
91 IF(ETB) 16,16,17
92 16 IF(TH.EQ.PAI/4.0) GO TO 55
93 WRITE(6,2006)
94 2006 FORMAT(1H ,111X,8H3RD MODE)
95 GO TO 53
96 55 WRITE(6,2007)
97 2007 FORMAT(1H ,111X,8H4TH MODE)
98 GO TO 53
99 17 II=2
100 GO TO 52
101 19 Q =(0.5*SWY*SIN(2.0*TH)+TCR*(1.0-SIN(2.0*TH)**2))*B*TW
102 WRITE(6,2008)
103 2008 FORMAT(1H ,111X,8H2ND MODE)
104 GO TO 53

```

---

```

105 56 CONTINUE

```

---

```

106 100 CONTINUE

```

---

```

107 STOP

```

---

```

108 END

```

---



---

Leere Seite  
Blank page  
Page vide